(21) Elemental analyses by Galbraith Laboratories, Inc., Knoxville, Tenn.
(22) J. V. Nef, *Justus Liebigs Ann. Chem.*, **308**, 264 (1899).
(23) J. König and V. Wolf, *Tetrahedron Lett.*, **19**, 1629 (1970).
(24) C. E. Castro, E. J. Gaughan, and D. C. Owsley, *J. Org. Chem.*, **30**, 587 (1965).
(25) V. P. Kravets, G. I Chervenyuk, and G. V. Grinev, *Zh. Org. Khim.*, **2**, 1244 (1966); *Chem. Abstr.*, **66**, 65231h (1967).
(26) C. F. Ward, *J. Chem. Soc.*, 2207 (1923).
(27) S. I. Miller, G. R. Ziegler, and R. Wieleseck in "Organic Syntheses", Collect. Vol. V, H. E. Baumgarten, Ed., Wiley, New York, N.Y., 1973, p 921.
(28) B. W. Howk and S. M. McElvain, *J. Am. Chem. Soc.*, **54**, 282 (1932).
(29) L. F. Fieser and K. L. Williamson, "Organic Experiments", 3rd ed, D. C. Heath, Boston, Mass., 1975, p 138.
(30) A. E. Bradfield, G. I. Davies, and E. Long, *J. Chem. Soc.*, 1389 (1949).

Two-Photon Spectroscopy of the Visual Chromophores. Evidence for a Lowest Excited $^1A_g^-$-Like $\pi\pi^*$ State in *all-trans*-Retinol (Vitamin A)

Robert R. Birge,* James A. Bennett,[1] Brian M. Pierce,[2] and Terry M. Thomas

Contribution from the Department of Chemistry, University of California, Riverside, California 92521. *Received May 23, 1977*

Abstract: A two-photon excitation maximum of *all-trans*-retinol (vitamin A) is observed approximately 1600 cm^{-1} to the red of the one-photon absorption maximum in EPA at 77 K. The observed state is "strongly allowed" in two-photon spectroscopy exhibiting a cross section at the 704-nm two-photon maximum of approximately 2×10^{-49} cm^4 s $molecule^{-1}$ $photon^{-1}$. The two-photon maximum is assigned to the lowest $\pi^* \leftarrow \pi$, "$^1A_g{}^{*-}$" $\leftarrow$ "$^1A_g{}^-$" transition on the basis of two-photon cross-section calculations using PPP-SCF-MO-CI wave functions including full single and double excitation configuration interaction. Torsional distortion and substituent effects associated with the β-ionylidene ring, while not altering the level ordering of the lowest energy "$^1B_u{}^*$" and "$^1A_g{}^{*-}$" $\pi\pi^*$ states, decrease the energetic separation of these two states relative to that observed in the analogous linear polyene, 2,10-dimethylundecapentaene.

The initial step in vertebrate vision involves the photochemical isomerization of the polyene aldehyde, 11-*cis*-retinal, which is bound to the opsin protein of rhodopsin via a protonated Schiff base linkage.[3] Characteristics of the visual chromophore that are important to its biophysical function include a high probability for photon absorption and a high quantum efficiency of cis → trans photoisomerization. Investigators have long recognized that these properties are characteristic of polyenes, but the photochemical origins of these properties are still not fully understood.[4]

The recent discovery of a lowest excited $^1A_g{}^{*-}$ $\pi\pi^*$ singlet state in linear polyenes[5-7] has prompted important revisions in our understanding of polyene electronic structure.[4-10] Prior to this discovery investigators had assigned the strongly allowed $^1B_u{}^* \leftarrow {}^1A_g$ transition as having the lowest energy. A lowest excited $^1A_g{}^{*-}$ $\pi\pi^*$ state has been reported in the high-resolution electronic absorption spectra of 1,8-diphenyloctatetraene[5,6] and 2,10-dimethylundecapentaene[7] and in the two-photon excitation spectra of diphenylpolyenes.[11,12] An identical level ordering in the visual chromophores, however, cannot automatically be assumed on the basis of these model compounds since little is known experimentally about the sensitivity of the $^1A_g{}^{*-}$-like ("$^1A_g{}^{*-}$")[13] state to conformational and electrostatic perturbations. In fact recent calculations predict that the ordering of the "$^1A_g{}^{*-}$" and "$^1B_u{}^*$" states in the visual chromophores is highly sensitive to conformation.[8] Since the photochemical behavior of the two states is predicted to be significantly different[8,14] an experimental determination of the level ordering is important to our understanding of polyene photochemistry both in solution and in the visual pigment.

In this paper we present a two-photon excitation spectrum which provides evidence that the "$^1A_g{}^{*-}$" state is 1600 cm^{-1} lower in energy than the "$^1B_u{}^*$" state in *all-trans*-retinol

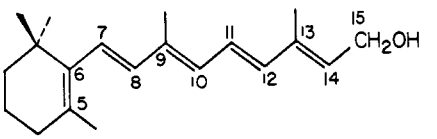

ALL-TRANS RETINOL

(vitamin A). Our assignment is based on a theoretical analysis indicating that only "$^1A_g{}^{*-}$" $\pi\pi^*$ states have significant two-photon cross sections in nonpolar polyenes at long wavelength (non-resonance-enhanced) regions of the spectrum. The out-of-plane distortion and substituent interaction associated with the β-ionylidene ring do not alter the level ordering of the lowest energy "$^1B_u{}^*$" and "$^1A_g{}^{*-}$" $\pi\pi^*$ states in *all-trans*-retinol. However, these substituent effects reduce the energy separation of these two states relative to that observed in the analogous linear polyene, 2,10-dimethylundecapentaene.[7]

Experimental Section

all-trans-Retinol was prepared by the sodium borohydride reduction of twice-recrystallized *all-trans*-retinal (Eastman Organic Chemicals) following the procedures of Hubbard.[15] The reduction was followed spectrophotometrically and the solute taken up in petroleum ether following reduced-pressure rotary evaporation of the ethanol. The petroleum ether was washed three times with distilled water and then removed under reduced pressure. The oil was then taken up in *n*-hexane and purified using thin layer chromatography on silica gel G using a solvent mixture of *n*-hexane and ethyl acetate (90:10 v/v). TLC purification was carried out in the dark under a nitrogen atmosphere. The solute was eluted with ethanol, filtered, and stored at liquid nitrogen temperature until used. Commercial preparations of *all-trans*-retinol contained a significant amount of luminescent impurities which produced spurious emission bands. Furthermore the nonanhydrous commercial preparations consistently proved more difficult to purify using TLC than were the synthesized samples.

0002-7863/78/1500-1533$01.00/0

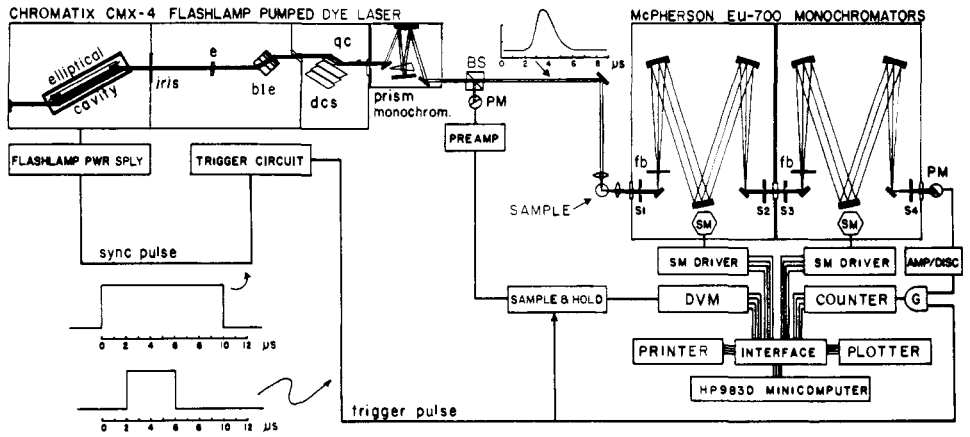

Figure 1. Tunable dye-laser excitation spectrometer. All two-photon excitation experiments were performed with the etalon (e) and field-stop baffles (fb) removed, the slits (S1–S4) adjusted to full aperture (2000 μ), the quartz crystal (qc) in place, the monochromator set at 480 nm [except when scanning the fluorescence spectrum to verify sample spectrum (see text)], and the prism monochromator set at the first harmonic to remove flashlamp output and trace second harmonic generation. All one-photon fluorescence and excitation experiments were performed as above but with the appropriate doubling crystal (dcs) in place and the prism monochromator set at the second harmonic. Remaining symbols are as follows: BS = beam splitter, PM = photomultiplier, SM = stepping motor, G = high-speed TTL gate.

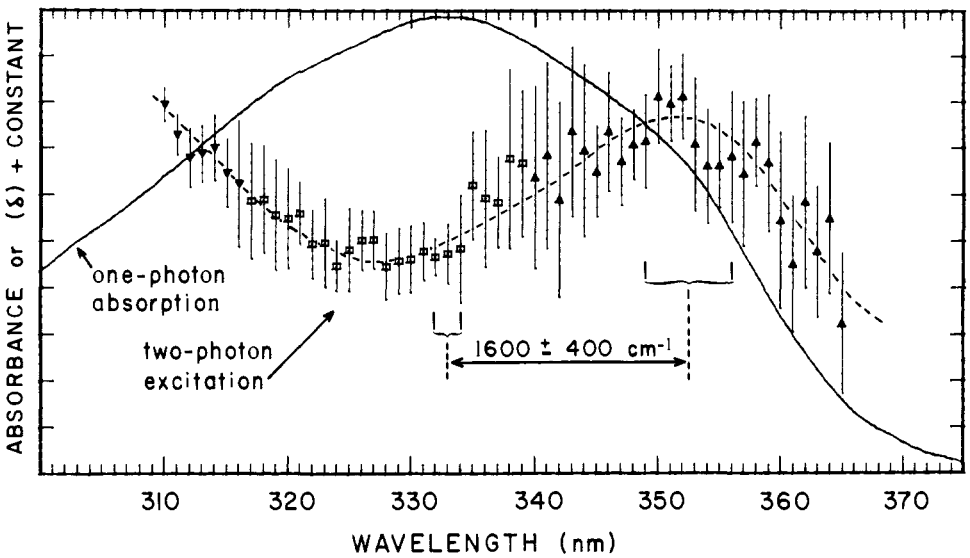

Figure 2. Comparison of the two-photon excitation spectrum (dotted line, vertical axis linear in cross section) and one-photon absorption spectrum (solid line, vertical axis linear in molar absorptivity) of *all-trans*-retinol in EPA at 77 K. The laser excitation wavelength is twice the wavelength indicated. The laser dyes used in the two-photon spectrum are indicated by symbol [▼ (Rhodamine 6G in 4% aqueous Ammonyx LO); □ (Rhodamine 640 in methanol-water (1:1 v/v)); ▲ (Oxazine 170 perchlorate in methanol-water (3:1 v/v))], with each symbol representing the average of 120 measurements (see Experimental Section). The height of the vertical line equals the standard deviation. The solute concentration was 6×10^{-6} M for the one-photon spectrum and 8×10^{-4} M for the two-photon spectrum.

The two-photon excitation spectrometer, shown in Figure 1, includes a 100-MHz gated-photon counting system and a computer controller and data acquisition system. The ability to average multiple scans and the use of gated photon counting techniques provided a significant improvement in the sensitivity of the spectrometer compared to conventional excitation spectrometers using analog detection and boxcar integration techniques.

The Chromatix CMX-4 flashlamp-pumped tunable dye laser was operated with a lamp voltage of 9 kV, which produced flashlamp energies of approximately 18 J per pulse and dye laser output energies of 2–8 mJ per pulse. Rhodamine 6G perchlorate (Eastman, 63 mg/L 4% aqueous Ammonyx LO), rhodamine 640 perchlorate (Exciton, 68 mg/L methanol-water, 1:1 v/v), and oxazine 170 perchlorate (Eastman, 38 mg/L methanol-water, 3:1 v/v) were used to cover the 620–730-nm wavelength range investigated (see Figure 2). The solutions of the latter two dyes were slightly acidified with a few drops of concentrated HCl.

The gated-photon counting system consisted of a 1P28 photomultiplier in an ambient temperature rf-shielded housing, a PAR Model 1121 100-MHz amplifier-discriminator operated in pulse-coincidence and internal-prescale modes, a high-speed TTL gate, and a 100-MHz counter. The laser excitation was monitored using analog sample-and-hold circuitry on a $5\frac{1}{2}$ digit DVM (see Figure 1) and was computationally corrected for photomultiplier response by the HP 9830 minicomputer. Each "measurement" represented the average of seven ratios of sample (fluorescence at 480 nm) divided by reference (laser intensity squared). Each data point in the spectrum shown in Figure 2 was obtained by taking 200 "measurements", discarding the highest and lowest 40, and taking an average of the remaining 120. This arbitrary approach minimized the problem of laser pulse amplitude instability which approached 30% at the high intensities and pulse repetition rates (15 or 30 pps) used in our experiments. At 5-nm intervals of the laser excitation wavelength the computer scanned the two-photon excited fluorescence spectrum to verify that the emission was associated with *all-trans*-retinol and not photoproducts (see Results and Discussion). The pulse width of the laser remained constant (fwhm = 1.2 μs) throughout the spectral range investigated.

An approximate value of the absolute two-photon cross section of *all-trans*-retinol at 704 nm was measured by comparing the fluorescence intensity of EPA solutions for two-photon (λ 704 nm) vs. one-

photon (λ′ 352 nm) excitation. The number of solute photons emitted per laser pulse following two-photon excitation, $N_{em}^{(2)}$, is given by

$$N_{em}^{(2)} = \frac{1}{2}\phi_{em}^{(2)} N_0^{(2)} \langle\delta_\lambda^{(2)}\rangle C^{(2)} I_0^{(2)} L \qquad (1)$$

where $\phi_{em}^{(2)}$ is the quantum efficiency for emission (fluorescence) for two-photon excitation, $N_0^{(2)}$ is the number of incident photons per laser pulse at λ 704 nm, $\langle\delta_\lambda^{(2)}\rangle$ is the two-photon cross section for two 704-nm photons in cm^4 s $molecule^{-1}$ $photon^{-1}$, $C^{(2)}$ is the concentration of *all-trans*-retinol in molecules cm^{-3}, $I_0^{(2)}$ is the laser intensity in photons cm^{-2} sec^{-1}, and L is the path length in cm. The corresponding equation for one-photon excitation is

$$N_{em}^{(1)} = \phi_{em}^{(1)} N_0^{(1)} [1 - \exp(-\langle\delta_\lambda^{(1)}\rangle C^{(1)} L)] \qquad (2)$$

where all variables are defined as in eq 1 except for $\langle\delta_\lambda^{(1)}\rangle$, which is the one-photon cross section in cm^2 $molecule^{-1}$. It is related to the decadic molar absorptivity, $\epsilon_{\lambda'}$, using

$$\langle\delta_\lambda^{(1)}\rangle = 1000 \ln 10 \epsilon_{\lambda'}/N_A = 3.8235 \times 10^{-21}\epsilon_{\lambda'} \qquad (3)$$

where N_A is Avogadro's number. The molar absorptivity of *all-trans*-retinol at 77 K in EPA was measured on a McPherson EU-700 double beam spectrometer (ϵ_{352} 35 400 L mol^{-1} cm^{-1}).

The two-photon cross section was calculated using

$$\langle\delta_\lambda^{(2)}\rangle = \left(\frac{N_{em}^{(2)}}{N_{em}^{(1)}}\right)\left\{\frac{2N_0^{(1)}[1 - \exp(-\langle\delta_\lambda^{(1)}\rangle C^{(1)} L)]}{N_0^{(2)} C^{(2)} I_0^{(2)} L}\right\} \qquad (4)$$

which was derived using eq 1 and 2 assuming $\phi_{em}^{(1)} = \phi_{em}^{(2)}$. This assumption is justified for molecules of low symmetry where different vibronic levels accessed by one-photon and two-photon excitation are expected to decay rapidly and radiationlessly to the lowest vibronic level of S_1. The apparatus used to measure $\langle\delta_\lambda^{(2)}\rangle$ was identical with that shown in Figure 1 with two exceptions. The 2.5-cm focal length lens near the sample was replaced with a 20-cm focal length lens which was adjusted to maintain a fairly constant beam diameter of 0.5 mm across the 5-mm path length cell. The beam splitter (BS) was removed and the laser intensity directly monitored by inserting a Gen-Tec ED-200 joulemeter in the laser beam behind the sample. Solute concentrations were necessarily different for the one-photon and two-photon experiment ($C^{(1)} = 1.2 \times 10^{14}$ molecule cm^{-3}, $C^{(2)} = 4.8 \times 10^{17}$ molecule cm^{-3}) with the former adjusted so that >99% of the 352-nm irradiation would be transmitted. The term $(N_{em}^{(2)}/N_{em}^{(1)})$ was directly measured as the ratio of the appropriate photon count rates of *all-trans*-retinol fluorescence at 495 nm since identical laser pulse rates and monochromator settings were used for both one-photon and two-photon excitation. The above procedure, however, contains many sources for error which are enumerated in Results and Discussion.

Spectra of *all-trans*-retinol were obtained in EPA (ethyl ether–isopentane–ethyl alcohol, 5:5:2 v/v) solvent using thin-walled 5-mm diameter quartz cells immersed in liquid nitrogen (77 K). Solutions were degassed by the freeze–pump–thaw method and cooled slowly to minimize cracking.

Theoretical

The two-photon cross section δ_{fo} (the superscript (2) is dropped in the following discussion) for a transition from the ground state (o) into some final state (f) is given by[16-19]

$$\delta_{fo} = \left[\frac{(2\pi e)^4}{(ch)^2}\right][\nu_\lambda \nu_\mu g(\nu_\lambda + \nu_\mu)]|S_{fo}(\lambda,\mu)|^2 \qquad (5)$$

where ν_λ is the frequency of the λ photon, ν_μ is the frequency of the μ photon, $g(\nu_\lambda + \nu_\mu)$ is the normalized line shape function (discussed below), and S_{fo} is given by

$$|S_{fo}(\lambda,\mu)|^2 = [\lambda_A \mu_B \lambda_R^* \mu_S^*][l_{A\alpha} l_{B\beta} l_{R\rho} l_{S\sigma}](S_{\alpha\beta} S_{\rho\sigma}^*) \qquad (6)$$

The first term on the right-hand side of eq 6 defines the polarization of the two photons where λ_A and μ_B are the Ath and Bth components of the polarization vectors of photons λ and μ. A and B can equal X, Y, or Z, the Cartesian coordinates of the laboratory. The second term on the right-hand side of eq 6 contains all the information about the molecular orientation of the absorbing molecule and is defined in terms of direction cosines, $l_{A\alpha}$, where A (or any capital Roman letter) defines the laboratory axis ($A = X$, Y, or Z) and α (any lower-case Greek letter) defines the molecular axis (α = x, y, or z). The last term on the right-hand side contains the molecular information and consists of a product of two second-rank tensors.[17]

$$S_{\alpha\beta} = \sum_i \left[\frac{\langle i|\alpha|o\rangle\langle f|\beta|i\rangle}{E_i - E_\lambda + i\Gamma} + \frac{\langle i|\beta|o\rangle\langle f|\alpha|i\rangle}{E_i - E_\mu + i\Gamma}\right] \qquad (7)$$

$\langle i|\alpha|o\rangle$ is the transition length along the α (molecular coordinate) axis for excitation from the ground state into state i, while $\langle f|\beta|i\rangle$ is the transition length along the β axis from state i into state f. E_i is the transition energy into state i and E_λ and E_μ are the energies of photon λ and photon μ, respectively. Γ is a damping constant appropriate for a typical excited state line width. A value of 0.05 eV is used in the calculations reported in this paper solely to prevent accidental resonances from producing unrealistically large cross sections.

The spectrometer used in the present investigation produces two-photon excitation using a single laser source. The energies of the λ and μ photons are identical, and a simple form for eq 6 can be obtained using the orientation averaging procedures of Monson and McClain.[17]

$$\delta_{fo} = \left[\frac{(2\pi e)^4}{(ch)^2}\right][\nu_\lambda^2 g(2\nu_\lambda)]|S_{fo}(\lambda,\lambda)|^2 \qquad (8)$$

$$|S_{fo}(\lambda,\lambda)|^2 = \sum_{\substack{i \\ (i\neq o,f)}}\sum_{\substack{j \\ (j\neq o,f)}} \left\{\frac{a[\langle i|\mathbf{r}|o\rangle \cdot \langle f|\mathbf{r}|i\rangle][\langle j|\mathbf{r}|o\rangle \cdot \langle f|\mathbf{r}|j\rangle]}{(E_i - E_\lambda)(E_j - E_\lambda) + \Gamma^2}\right.$$

$$+ \frac{b[\langle i|\mathbf{r}|o\rangle \cdot \langle j|\mathbf{r}|o\rangle][\langle f|\mathbf{r}|i\rangle \cdot \langle f|\mathbf{r}|j\rangle]}{(E_i - E_\lambda)(E_j - E_\lambda) + \Gamma^2}$$

$$\left. + \frac{b[\langle i|\mathbf{r}|o\rangle \cdot \langle f|\mathbf{r}|j\rangle][\langle f|\mathbf{r}|i\rangle \cdot \langle j|\mathbf{r}|o\rangle]}{(E_i - E_\lambda)(E_j - E_\lambda) + \Gamma^2}\right\} \qquad (9)$$

Various photon polarization relationships can be defined in terms of the polarization constants a and b. Our experimental conditions produce both photons linearly polarized with parallel polarization ($a = b = 8$). Other relationships are defined in the footnotes to Table I.

The line shape function, $g(\nu_\lambda + \nu_\mu)$, which appears in eq 5 and 8 is proportional to the cross-sectional contour of the final state and is defined such that the integral over all frequency space is normalized to unity. The broad, structureless absorption bands in the visual chromophores are very nearly Gaussian in profile and we will represent the line shape function as a Gaussian profile centered at ν_f, where ν_f is the frequency maximum for two-photon excitation into state f.

$$g(2\nu_\lambda) = g_{max} \exp\left\{\frac{-4 \ln 2}{(\Delta\nu)^2}[2\nu_\lambda - \nu_f]^2\right\} \qquad (10)$$

where

$$g_{max} = [4 \ln 2/\pi(\Delta\nu)^2]^{1/2} \cong 1/(1.0645\Delta\nu) \qquad (11)$$

Consequently for a given two-photon absorption bandwidth ($\Delta\nu$ = fwhm) the maximum value for $g(2\nu_\lambda)$ will equal g_{max} (eq 11). The calculations presented in Results and Discussion use a g_{max} of 5×10^{-15} s corresponding to a typical retinyl polyene fwhm of 6000 cm^{-1}.[20]

The state energies and transition lengths required for the evaluation of eq 8 were calculated using Pariser–Parr–Pople SCF–MO–CID procedures.[8] The transition energies of the excited states were calculated relative to the uncorrelated ground state following the approach and rationale of ref 8. The values are listed in the ΔE columns of Tables I and II. The energy of the incident photons, E_λ, was determined by dividing the appropriate final state transition energy by 2. Resonance and near resonance effects were not important until the energy of the final state was within 1.5 eV of twice the energy of the

Table I. Calculated One-Photon Oscillator Strengths and Two-Photon Cross Sections for the Lowest Lying $\pi^* \leftarrow \pi$ Transitions in *all-trans*-Retinol[a]

ΔE, eV[b]	Sym[c]	f[d]	$\lvert\theta^e\rvert$	$\langle A\rangle^f$	$\langle B\rangle^g$	$\langle C\rangle^h$	$\langle D\rangle^i$	Ω^j
3.233	"$^1A_g^-$"	5.9E − 08	24	2.915	1.115	2.229	1.800	0.765
3.481	"^1B_u"	1.061	9	0.000	0.000	0.000	0.000	
3.981	"^1B_u"	2.4E − 06	7	0.299	0.103	0.207	0.196	0.690
4.536	"$^1A_g^-$"	1.6E − 06	69	2.491	0.877	1.755	1.613	0.704
4.883	"$^1A_g^-$"	5.2E − 05	66	0.627	0.200	0.399	0.427	0.637
5.061	"$^1A_g^+$"	0.101	65	0.001	0.000	0.001	0.000	
5.281		1.0E − 05	38	(22)	(8)	(15)	(14)	0.705
5.722		3.5E − 07	21	(2.557)	(0.774)	(1.549)	(1.783)	0.606
6.069		3.1E − 06	67	(4070)	(1358)	(2716)	(2712)	0.667

[a] Based on PPP-SCF-MO-CI calculations including full single and double excitation CI (see text). Polyene chain is all-trans except for C_6-C_7 bond which is s-cis (45°). Standard bond lengths are assumed ($R_{C=C}$ = 1.35 Å, R_{C-C} = 1.46 Å). The two-photon cross sections [in units of cm^4 s molecule^{-1} photon^{-1} ($\times 10^{48}$)] are calculated assuming $g_{max} = 5 \times 10^{-15}$ s, Γ = 0.05 eV, and $E_\lambda = E_\mu = \Delta E/2$. Cross sections given in parentheses are significantly enhanced through resonance. [b] Transition energy relative to uncorrelated ground state (see ref 8). [c] Approximate symmetry of electronic state. [d] Oscillator strength of one-photon transition. [e] Polarization of one-photon transition relative to a line connecting the C_6 carbon with the C_{14} carbon. [f] Cross section for both photons linearly polarized with parallel polarization ($a = b = 8$ in eq 9). [g] Cross section for both photons linearly polarized with perpendicular polarization or one photon circularly polarized, the other linearly polarized perpendicular to the plane of circular polarization ($a = -4$, $b = 6$ in eq 9). [h] Cross section for both photons circularly polarized in the same sense with parallel propagation ($a = -8$, $b = 12$ in eq 9). [i] Cross section for both photons circularly polarized in the opposite sense with parallel propagation ($a = 12$, $b = 2$ in eq 9). [j] Polarization ratio of the two-photon transition defined as $\langle C\rangle/\langle A\rangle$.

Table II. Calculated One-Photon Oscillator Strengths and Two-Photon Cross Sections for the Lowest Lying $\pi^* \leftarrow \pi$ Transitions in *all-trans*-Retinal[a]

ΔE, eV[b]	Sym[c]	f[d]	$\lvert\theta^e\rvert$	$\langle A\rangle^f$	$\langle B\rangle^g$	$\langle C\rangle^h$	$\langle D\rangle^i$	Ω^j
3.172	"$^1A_g^-$"	0.251	9	2.993	1.037	2.074	1.956	0.693
3.411	"^1B_u"	0.965	12	1.417	0.481	0.962	0.935	0.679
4.052	"^1B_u"	1.1E − 03	39	0.310	0.123	0.246	0.187	0.794
4.703	"^1A_g"	2.4E − 03	43	7.144	2.486	4.972	4.657	0.696
4.977	"$^1A_g^+$"	0.030	88	7.468	2.511	5.023	4.957	0.673
5.081	"^1B_u"	1.2E − 03	89	(4.821)	(1.584)	(3.168)	(3.237)	0.657
5.421		6.0E − 03	45	(53)	(18)	(36)	(35)	0.683
5.465		9.0E − 04	46	(51)	(18)	(36)	(33)	0.701
5.775		3.0E − 03	45	(499)	(166)	(332)	(333)	0.665

[a] Based on PPP-SCF-MO-CI wave functions including full single and double excitation CI (see text). The crystal geometry of T. Hamanaka, T. Mitsui, T. Ashida, and M. Kakudo, *Acta Crystallogr., Sect. B*, **28**, 214 (1972), is assumed. The two-photon cross section [in units of cm^4 s molecule^{-1} photon^{-1} ($\times 10^{48}$)] are calculated assuming $g_{max} = 5 \times 10^{-15}$ s, Γ = 0.05 eV, and $E_\lambda = E_\mu = \Delta E/2$. Cross sections given in parentheses are significantly enhanced through resonance. [b-j] See Table I.

lowest lying singlet state. Since the calculated transition energies are accurate to less than 0.5 eV, the two-photon cross sections calculated for resonantly enhanced states must be considered very approximate. These values are enclosed in parentheses in Tables I and II. Repulsion integrals over atomic orbitals were calculated using the Ohno approximation[21] and all possible single and double excitations from the SCF ground state were included in the CI Hamiltonian. It has previously been shown that double excitation CI is a prerequisite for the accurate prediction of the relative $^1A_g{}^{*-}$ and $^1B_u{}^*$ level orderings in both linear[9,10] and retinyl[8,14] polyenes. A detailed examination of the PPP-CID formalism is presented in ref 22.

Results and Discussion

Calculations of the two-photon cross sections of the low-lying $\pi\pi^*$ states of *all-trans*-retinol and *all-trans*-retinal are shown in Tables I and II. Various photon polarization relationships are compared in columns $\langle A\rangle$, $\langle B\rangle$, $\langle C\rangle$, and $\langle D\rangle$. As can be seen the strongest two-photon absorption is predicted to occur for the coparallel linear polarization used in the present investigation ($\langle A\rangle$). The table for *all-trans*-retinal is included to demonstrate the predicted effect of molecular polarity on the two-photon spectrum. Whereas only "$^1A_g{}^{*-}$" $\pi\pi^*$ states have significant cross sections in *all-trans*-retinol, the symmetry breakdown associated with the carbonyl group of retinal mixes "$^1A_g{}^{*-}$" character into all of the excited states of *all-trans*-retinal which considerably complicates the predicted spectrum. The possible interpretative problems associated with these effects as well as the wavelength-dependent quantum yield of retinal prompted our choice of retinol for this initial investigation.[23,24]

Examination of Tables I and II indicates that all of the allowed two-photon transitions have virtually identical polarization ratios (defined as the ratio of the cross section induced by circularly polarized $\langle C\rangle$ vs. linearly polarized $\langle A\rangle$ light). This observation is not surprising since only "$^1A_g{}^{*-}$" states are two photon allowed in polyenes, but it is disappointing from a diagnostic standpoint.

The two-photon cross section maximum for the lowest lying "$^1A_g{}^{*-}$" ← "$^1A_g^-$" transition in *all-trans*-retinol is calculated to be 2.92 × 10^{-48} cm^4 s molecule^{-1} photon^{-1} for linearly polarized light. This value represents an extremely strong two-photon absorption, and, as we discuss below, is probably at least one order of magnitude too large.[25] The major contribution to the calculated two-photon cross section is due to a single intermediate level, the low-lying strongly allowed "$^1B_u{}^*$" state. We can write eq 9 in the following form and account for approximately 90% of the calculated cross section in the lowest excited "$^1A_g{}^{*-}$" state in both *all-trans*-retinol and *all-trans*-retinal. The ground state is indicated in eq 11

$$|S_{^1A_g{}^{-}\leftarrow S_0}(\lambda,\lambda)|^2 = \frac{(a+b)[\langle {}^1B_u|\mathbf{r}|S_0\rangle \cdot \langle {}^1A_g{}^-|\mathbf{r}|{}^1B_u\rangle]^2}{(E_{^1B_u} - E_\lambda)^2} + \frac{b|\langle {}^1B_u|\mathbf{r}|S_0\rangle|^2|\langle {}^1A_g{}^-|\mathbf{r}|{}^1B_u\rangle|^2}{(E_{^1B_u} - E_\lambda)^2} \quad (11)$$

by S_o (rather than $^1A_g^-$), excited state asterisks are dropped, and the damping constant, Γ, is ignored. The contribution of the intermediate "^1B_u*" state will be most significant when the transition length between the "^1A_g*$^-$" and "^1B_u*" states is large and the transition length vectors $\langle {}^1B_u|\mathbf{r}|S_o\rangle$ and $\langle {}^1A_g^-|\mathbf{r}|{}^1B_u\rangle$ are similarly polarized. The above criteria are fully satisfied in the case of both *all-trans*-retinol[26] and *all-trans*-retinal and are responsible for the large calculated cross sections.

The two-photon excitation spectrum of *all-trans*-retinol is shown in Figure 2. The following observations are important to the correct interpretation of this spectrum.

(1) A considerable amount of the laser irradiation is scattered into the monochromator due to our use of a low-temperature, optically imperfect solvent glass. The weak emission which is characteristic of two-photon induced fluorescence required adjusting the monochromators for large spectral bandwidth (40 Å) and permitted some scattered light to reach the detector. A portion of the two-photon excitation intensity in the 305–320-nm region may be due to scattered laser light since a slight deviation from the power-squared dependence was observed in this region.

(2) At 5-nm intervals, the computer automatically scanned the two-photon induced emission spectrum to assure that the excitation spectrum was associated with *all-trans*-retinol. In all cases, the (uncorrected) fluorescence maximum occurred at 495 nm and the emission spectrum corresponded within experimental error to the laser excited one-photon fluorescence spectrum generated by inserting the appropriate doubling crystal (see Figure 1). The two-photon excitation spectrum in Figure 2 was observed by sampling the fluorescence off-maximum at 480 nm to reduce scattered light interference.

(3) The problems of what appeared to be in situ second harmonic generation in the sample cell were minimized by using thin-walled quartz 5-mm sample tubes, focusing the laser to the center of the sample cell, and vertically adjusting the sample cell so that the beam intercepted the most transparent portion of the solvent glass. The "two-photon" excitation maximum occassionally shifted to higher energy when these precautions were not observed. Although we interpret this "blue shift" as due to the solute's absorption of a single photon subsequent to in situ second harmonic generation, other explanations are possible.[27]

(4) The concentration dependence of the two-photon excitation maximum at 350 nm and the two-photon induced fluorescence spectrum [see (2) above] both indicate that the 350-nm spectral feature is due to monomer (and not to dimer or *n*-mer) *all-trans*-retinol. The fluorescence intensity displayed the correct power-squared dependence throughout the wavelength range investigated with the exception of the 302–320-nm range noted in (1).

(5) The inherent difficulties in measuring two-photon cross sections due to inhomogeneities of the laser beam,[17] self-focusing and thermal lens effects,[28] the experimental difficulties of accurately focusing the beam to a well-defined spot size, and a host of other potential problems[29,30] prevented our measuring $\langle\delta\rangle$ with absolute accuracy using eq 4. Our experimental measurements fall into the range $(2.5 \pm 1.6) \times 10^{-49}$ cm^4 s molecule^{-1} photon^{-1} at 704 nm (2 × 352 nm). Considering the above sources for error, however, this value should be considered absolute only to within one order of magnitude. The experimental values are roughly one order of magnitude smaller than the calculated values listed in Table I.

The above experimental observation, when evaluated in terms of our calculations, supports the assignment of the 350-nm two-photon maximum to the "^1A_g*$^-$" ← "$^1A_g^-$" transition. This assignment indicates that the "^1A_g*$^-$" state of *all-trans*-retinol is approximately 1600 cm^{-1} lower in energy than the strongly allowed "^1B_u*" state (see Figure 2). This separation in maxima has the same sign but is significantly smaller in magnitude than the 3100-cm^{-1} system origin separation between the "^1B_u*" and "^1A_g*$^-$" states in 2,10-dimethylundecapentaene.[7] We must be cautious in interpreting this difference. The environmental perturbations of a 4.2 K *n*-nonane matrix and a 77 K EPA glass are potentially quite different and the smaller splitting in retinol could result from environmental rather than molecular differences. Fortunately, a 77 K low-resolution spectrum of the "^1A_g*$^-$" ← "$^1A_g^-$" transition in undecapentaene has also been reported in EPA,[7b] where an origin separation of 3250 cm^{-1} between the "^1B_u*" and "^1A_g*$^-$" states was observed. The 150-cm^{-1} difference in the state splitting observed in the 4 K *n*-nonane matrices vs. the 77 K EPA glass lies within the experimental error of band assignments in EPA.[7b] We conclude that solvent effects are not responsible for the observed differences in *all-trans*-retinol (maxima) vs. undecapentaene (origin) "^1B_u*"-"^1A_g*$^-$" splitting.

A potentially more important effect involves the differences in the Franck–Condon factors for excitation into the "^1B_u*" vs. "^1A_g*$^-$" states. The degree of bond-order reversal in the "^1A_g*$^-$" state is expected to be larger than that in the "^1B_u*" state resulting in an increase in the Franck–Condon factors in the higher vibrational levels of the former, vs. the latter, excited state. The importance of these effects can clearly be seen in a comparison of the vibronic intensities in the absorption and emission spectra of undecapentaene.[7b] However, the high degree of inhomogeneous broadening present in the electronic spectra of retinyl polyenes has been shown to decrease the importance of this effect.[31,32]

We conclude that the effect of Franck–Condon factors on shifting the absorption maxima (relative to the system origins) in the "^1A_g*$^-$" state relative to the "^1B_u*" state produces less than a 1000-cm^{-1} difference between the two states.[31] Accordingly, roughly one-half of the 3000- to 1600-cm^{-1} difference between undecapentaene origin splitting vs. *all-trans*-retinol maxima splitting is due to a genuine decrease in the energy separation of these states in *all-trans*-retinol. This decrease in "^1A_g*$^-$"-"^1B_u*" splitting in retinol is probably due to the nonplanar 6-s-cis linkage and inductomesomeric effects associated with the β-ionylidene ring. The freely rotating hydroxyl group is not expected to significantly affect the $\pi\pi$* states, and this conclusion is supported by the lack of sensitivity of the "^1B_u*" ← "$^1A_g^-$" transition to solvent polarity.

Comments and Conclusions

(1) *all-trans*-Retinol has a lowest excited "^1A_g*$^-$" $\pi\pi$* state approximately 1600 cm^{-1} lower in energy than the strongly allowed "^1B_u*" state in an EPA glass at 77 K. The "^1A_g*$^-$" state is "strongly allowed" in two-photon spectroscopy exhibiting a cross section at the 704-nm two-photon maximum of approximately 2×10^{-49} cm^4 s molecule^{-1} photon^{-1}. Although the presence of the β-ionylidene ring does not alter the level ordering of the lowest "^1B_u*" and "^1A_g*$^-$" $\pi\pi$* states, it does decrease the energy separation of these two states relative to that observed in 2,10-dimethylundecapentaene.

(2) Theoretical calculations predict that the low-lying "^1A_g*$^-$" state should be strongly two-photon allowed in virtually all polyenes, whether polar, nonpolar, linear, or nonlinear, provided that a strongly one-photon allowed "^1B_u*" state is nearby (see discussion associated with eq 8 and ref 33). It is possible that the difficulty in observing the ^1A_g*$^-$ ← $^1A_g^-$ transition in butadiene[34] and hexatriene[35] using multiphoton ionization techniques is associated with nearby Rydberg states with such large two-photon cross sections that they dominate the spectral region of interest.[34,35]

Acknowledgments. This work was supported in part by the donors of the Petroleum Research Fund, administered by the

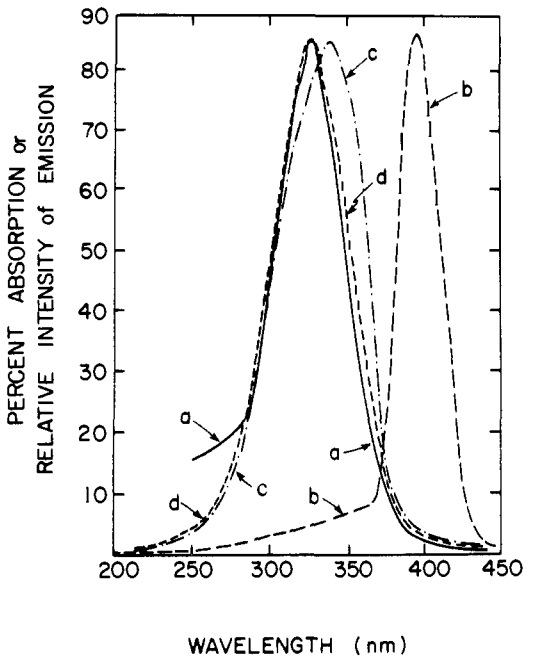

Figure 3. The effect of solute concentration and instrumental factors on the one-photon excitation spectrum of *all-trans*-retinol in EPA at 77 K. The one-photon absorption is shown for comparison in spectrum a. The excitation spectra were taken on an Aminco-Bowman spectrofluorimeter using a 5-mm diameter cell, 0.5-mm slit widths on both excitation and emission sides of the cell, and a 200-W xenon lamp excitation source. Concentrations for the excitation spectra are 10^{-3} (b), 10^{-5} (c), and 10^{-7} M (d). Emission was monitored at 500 nm.

American Chemical Society, Research Corporation, and the Committee on Research, University of California, Riverside. J.A.B. gratefully acknowledges that his graduate student summer fellowship was supported by the James Thurber Memorial Fund of Fight For Sight, Inc., New York. The authors wish to thank Professors Ronald Christensen, Mostafa El-Sayed, Bruce Hudson, David Kliger, Bryan Kohler, and Arieh Warshel for interesting and helpful discussions, and Professor Martin Karplus and Dr. Klaus Schulten for their contributions to the molecular orbital portions of this research. R.R.B. gratefully acknowledges a University of California Regents Faculty Fellowship.

Appendix. Wavelength Independence of Quantum Yield in Retinol

The two-photon excitation spectrum shown in Figure 2 was calculated assuming a wavelength-independent quantum yield of fluorescence, ϕ_f, for *all-trans*-retinol. The purpose of this section is to verify the intrinsic wavelength independence of ϕ_f, to comment on the instrumental factors that can lead to an observed wavelength dependence, and to demonstrate that instrumental factors *were not* responsible for shifting the two-photon excitation maximum to the red of the one-photon absorption maximum.

The influence of instrumental factors on the observed one-photon excitation spectrum of *all-trans*-retinol has been discussed by Kahan.[36] At high concentrations the solute absorption band can red shift the transversely monitored excitation spectrum by absorbing a significant percentage of the irradiation over a small path length as shown in Figure 3. At sufficiently low solute concentrations, however, the one-photon absorption (spectrum a of Figure 3) and excitation (spectrum d) spectra correspond within experimental error from 300 to 400 nm (see also ref 36). This observation indicates that the intrinsic fluorescence quantum yield is wavelength independent within the wavelength region studied in the present investigation.

Nevertheless, a cursory examination of Figure 2 might suggest that concentration effects (self-absorption) are responsible for the red shift in the two-photon excitation spectrum. We can categorically rule out this possibility, however, by applying Beer's law to the one-photon vs. two-photon absorption processes. The three solute concentrations investigated in Figure 3 will individually absorb the following percentages of the incident radiation at λ_{max} (332 nm) over a 5-mm path length: >99.9% (10^{-3} M, curve b); 63% (10^{-5} M, curve c); 0.6% (10^{-7} M, curve d). If we assume, for illustration purposes, a maximum two-photon cross section of 10^{-48} [much larger than observed for *all-trans*-retinol (see Results and Discussion)], and the experimental conditions of the present investigation (see Experimental Section), the above concentrations will absorb the following maximum percentages of the incident two-photon radiation over a 5-mm path length: $<10^{-4}$% (10^{-3} M; the concentration used for the two-photon excitation experiment was 8×10^{-4} M); $<10^{-8}$% (10^{-5} M); $<10^{-10}$ % (10^{-7} M). These values are all significantly smaller than the 0.6% value demonstrated to be sufficient for removing self-absorption effects under one-photon excitation conditions. Furthermore, the geometrical arrangement used in the two-photon experiment (Figure 1) is less sensitive to concentration effects than that used in the one-photon investigation (see caption of Figure 3). We can therefore eliminate the possibility that the red shift in the two-photon maximum relative to the one-photon maximum shown in Figure 2 resulted from concentration effects.

References and Notes

(1) University of California Regents Graduate Student Fellow, 1976–present, and Fight-For-Sight Graduate Student Fellow, summer 1977.
(2) National Science Foundation Undergraduate Research Participant, summer 1976, and Fight-For-Sight Undergraduate Fellow, summer 1977.
(3) D. Bownds, *Nature (London)*, **216**, 1178 (1967); G. Wald, *Science*, **162**, 230 (1968); W. J. DeGrip et al., *Biochem. Biophys. Acta*, **303**, 189 (1973); A. R. Oseroff and R. H. Callender, *Biochemistry*, **13**, 4243 (1974).
(4) B. S. Hudson and B. E. Kohler, *Annu. Rev. Phys. Chem.*, **25**, 437 (1974), and references, cited therein.
(5) B. S. Hudson and B. E. Kohler, *Chem. Phys. Lett.*, **23**, 139 (1973).
(6) B. S. Hudson and B. E. Kohler, *J. Chem. Phys.*, **59**, 4984 (1973).
(7) (a) R. L. Christensen and B. E. Kohler, *J. Chem. Phys.*, **63**, 1837 (1975); (b) *Photochem. Photobiol.*, **18**, 293 (1973).
(8) R. R. Birge, K. Schulten, and M. Karplus, *Chem. Phys. Lett.*, **31**, 451 (1975).
(9) K. Schulten and M. Karplus, *Chem. Phys. Lett.*, **14**, 305 (1972).
(10) K. Schulten, I. Ohmine, and M. Karplus, *J. Chem. Phys.*, **64**, 4422 (1976).
(11) R. L. Swofford and W. M. McClain, *J. Chem. Phys.*, **59**, 10 (1973).
(12) G. R. Holtom and W. M. McClain, *Chem. Phys. Lett.*, **44**, 436 (1976).
(13) Symmetry classifications given in quotation marks are approximate and are derived by correlating the properties of a given electronic state with those of the analogous state in a linear polyene of C_{2h} symmetry. In other words, "$^1A_g^{*-}$" should be interpreted as $^1A_g^{*-}$-like.
(14) R. R. Birge, K. Schulten, B. Klahn, D. S. Kliger, and M. Karplus, to be published.
(15) R. Hubbard, *J. Am. Chem. Soc.*, **78**, 4662 (1956).
(16) The interested reader should refer to the excellent paper by Monson and McClain[17] for a more complete discussion of the theoretical treatment presented here.
(17) P. R. Monson and W. M. McClain, *J. Chem. Phys.*, **53**, 29 (1970).
(18) W. M. McClain, *Acc. Chem. Res.*, **7**, 129 (1974).
(19) W. L. Peticolas, *Annu. Rev. Phys. Chem.*, **18**, (1967).
(20) W. S. Sperling in "Biochemistry and Physiology of Visual Pigments", H. Langer, Ed., Springer-Verlag, New York, N.Y., 1973, p 19.
(21) K. Ohno, *Theor. Chim. Acta*, **2**, 219 (1964).
(22) R. R. Birge, K. Schulten, and M. Karplus, to be published.
(23) The problem of two-photon excitation into the $n\pi^*$ state might also complicate the spectrum.[24]
(24) R. A. Harris, *Chem. Phys. Lett.*, **19**, 201 (1973).
(25) The inaccuracy of our calculations on low-lying excited states is due primarily to our use of semiempirical PPP–SCF–MO–CI wave functions and the tendency of these calculations to overestimate the transition length integrals. Small errors in the calculated transition lengths are greatly magnified because of the fourth-order dependence of the numerator (eq 9). An additional source of error occurs for higher energy excited states where inaccuracies in the calculated transition energies are magnified due to near-resonance effects.
(26) Our PPP–SCF–MO–CI wave functions (see footnote *a*, Table I) calculate the following integrals for *all-trans*-retinol: $|\langle {}^1B_u^* | \mathbf{r} | {}^1A_g^{*-} \rangle| = 0.7142$ Å, $|\langle {}^1B_u^* | \mathbf{r} | S_0 \rangle| = 1.8662$ Å, with an angle of 31° between the two transition length vectors.
(27) One referee suggested that the observed behavior might be associated

with dielectric breakdown due to light trapped in the cracks of the fractured sample.
(28) R. D. Drucker and W. M. McClain, *J. Chem. Phys.*, **61**, 2609 (1974).
(29) S. Speiser and S. Kimel, *J. Chem. Phys.*, **51**, 5614 (1969).
(30) J. P. Hermann and J. Ducuing, *Phys. Rev., Sect. A*, **5**, 2557 (1972).
(31) A dramatic example of the effect of inhomogeneous broadening on the absorption and emission envelopes can be seen in Figure 5 of ref 7b in which the spectra of undecapentaene and axerophtene are compared. Axerophtene, a retinyl polyene with a terminal β-ionylidene ring identical with that in *all-trans*-retinol, exhibits almost mirror image symmetry in its absorption and emission bands. The mirror image symmetry of *all-trans*-retinol absorption and emission spectra has been analyzed by Thomson, who observed a mismatch of roughly 900 cm^{-1} in the mirror-image superimposed spectra.[32]
(32) A. J. Thomson, *J. Chem. Phys.*, **51**, 4106 (1969).
(33) R. R. Birge and B. M. Pierce, to be published.
(34) P. M. Johnson, *J. Chem. Phys.*, **64**, 4638 (1976).
(35) D. H. Parker, S. J. Sheng, and M. A. El-Sayed, *J. Chem. Phys.*, **65**, 5534 (1976).
(36) J. Kahan, *Acta Chem. Scand.*, **21**, 2515 (1967).

Nuclear Magnetic Resonance Studies of Catecholamines. Complex Formation with Adenosine 5′-Triphosphate in Aqueous Solution. Stoichiometry and Molecular Conformations

Joseph Granot

Contribution from the Department of Structural Chemistry, The Weizmann Institute of Science, Rehovot, Israel. *Received June 23, 1977*

Abstract: ^1H NMR investigation of the association between catecholamines (dopamine, norepinephrine, epinephrine) and ATP have been undertaken in order to elucidate the stoichiometry and the structure of their complexes in aqueous solution. Analysis of the changes in the chemical shifts upon complexation of the molecules involved confirm that the main catecholamine–ATP complexes formed have stoichiometries of 1:1 and 2:1, with stepwise formation constants of 16 M^{-1} and 10 M^{-1}, respectively. These complexes are stabilized by ring association, via vertical stacking and hydrogen bond formation between the catechol hydroxyls and the purine nitrogens, and electrostatic interaction between the protonated ammonium group (at pD 6.9) and the negative phosphate moiety. The hydrogen bonds are found to be weak, and it is suggested that they are solvent mediated. Concentrations of complexes of higher stoichiometries, in which the association involves chain interaction alone, are found to be practically negligible. A marked increase (of ~30%) in the population of the trans conformer about the C_α–C_β bond of dopamine due to complexation with ATP is inferred from changes in the vicinal proton spin coupling constants. The ribose ring of ATP, existing as a $^2E \leftrightharpoons {}^3E$ equilibrium with preference for the ^2E pucker, is found to display significant increase (of ~15%) in the population of the ^3E conformation upon complexation with catecholamines. Intermolecular geometries of the 1:1 and 2:1 complexes, compatible with the experimental results, are derived by means of a ring-current shift analysis.

The occurrence of ATP in storage sites of catecholamines, as well as its participation in the processes of uptake and release of catecholamines in biological organelles, indicate the importance of the association between these compounds. In a previous paper[1] a qualitative study of the interactions between catecholamines and adenine nucleotides has been reported. It has been shown that their association in aqueous solution (at pD ~7) involves mainly ring (purine and catechol) stacking. In addition the side chains also interact through electrostatic attraction between the positive ammonium group and the negative phosphate moiety. It has also been suggested that catecholamine nucleotide complexes of 1:1 and of 2:1 stoichiometries would be the prevalent complexes.

In the present work further, quantitative characterization of the catecholamine–ATP system is provided. The stoichiometries of the binary complexes have been established and the appropriate formation constants were derived. The structures of the complexes were determined through ring-current shift analysis. Changes in spin coupling constants were interpreted in terms of variations in the intramolecular conformations. The measurements were performed at pD 6.9. In the region of this pD the interactions between the catecholamines and ATP were found to be most pronounced.[1] Also this pD value is not close to the pK_as of either the adenine ring[2] or of the hydroxyl and ammonium groups of the amines;[3] thus, any complications due to acid–base reactions were avoided.

Experimental Section

Materials. Amines[4] and adenine nucleotides of highest purity were obtained from Sigma Chemical Co. Experimental solutions were made up by dissolving the materials in D_2O (99.7%).

NMR Spectra. ^1H NMR chemical shifts were measured on a Bruker HFX-10 spectrometer operating at 90 MHz (except for the shifts of the ATP ribose protons which were measured at 270 MHz to allow unambiguous assignment of the resonances and to avoid the considerable overlap occurring at 90 MHz). A trace of dioxane in the experimental solutions served as internal reference for for shift measurements. Upfield shifts (expressed in Hertz) are denoted by positive sign. Each measurement has been repeated three–four times to reduce random errors. The experimental uncertainty in the shift measurements is thus estimated as ±0.5 Hz. Spin coupling constants were measured on a Bruker WH-270 spectrometer, equipped with a Nicolet Model 1180 32K computer, operating at 270 MHz in the Fourier transform mode. All the measurements have been performed at an ambient probe temperature of 27 °C.

The notation of the proton resonances of the studied amines is as given in Table I of ref 1.

Calculation of Concentrations of Complexes. Analysis of NMR data (e.g., chemical shifts, relaxation times) for determination of stability constants requires expressions for the equilibrium concentrations of the various species present in the experimental solution in terms of these parameters. Referring to the case of binary complexes, a central compound (A) with a maximum complexation number N, would bind ligand molecules (L) to form a series of complexes AL, $AL_2 \cdots AL_N$ by N successive steps. The nth consecutive formation constant is thus defined by the mass law equation

$$AL_{n-1} + L \rightarrow AL_n \quad K_n = [AL_n]/[AL_{n-1}][L] \qquad (1)$$

If we let $A = [A]$ and $L = [L]$ denote the concentrations of the free components, and $L_n = [AL_n]$ for $n = 1, N$ denote the concentrations

0002-7863/78/1500-1539$01.00/0